Journal of Computational Mathematics, Vol.22, No.3, 2004, 407–426.

THE ARTIFICIAL BOUNDARY CONDITIONS FOR NUMERICAL SIMULATIONS OF THE COMPLEX AMPLITUDE IN A COUPLED BAY-RIVER SYSTEM *[1)]

Hou-de Han Xin Wen
(*Department of Mathematical Sciences, Tsinghua University, Beijing 100084, China*)

Abstract

We consider the numerical approximations of the complex amplitude in a coupled bay-river system in this work. One half-circumference is introduced as the artificial boundary in the open sea, and one segment is introduced as the artificial boundary in the river if the river is semi-infinite. On the artificial boundary a sequence of high-order artificial boundary conditions are proposed. Then the original problem is solved in a finite computational domain, which is equivalent to a variational problem. The numerical approximations for the original problem are obtained by solving the variational problem with the finite element method. The numerical examples show that the artificial boundary conditions given in this work are very effective.

Mathematics subject classification: 65N05, 76B20.
Key words: Coupled bay-river system, Complex amplitude, Artificial boundary conditions, Finite element method.

1. Introduction

This paper is to solve the two-dimensional complex amplitude in a coupled bay-river system. Consider a bay located at a river mouth and connected to the open sea through a narrow entrance(see Figure 1). Such a coupled bay-river system, may be agitated into resonant states by external oscillations with particular periods. The water depth everywhere in the domain is assumed to be constant, and the solid boundary is considered to be impermeable. The model river possesses an invariant cross section, and the length of river could be either semi-infinite or finite. In these two cases, the non-reflective and perfect reflective conditions will be used in the end of the river respectively. Additionally, the width of the river and the bay entrance are assumed to be small compared with both the dimension of the bay and the wavelength.

The river mouth , bay entrance and coastline are defined by

$$\begin{aligned}\Gamma_{rm} &= \{(-a,y)|-\frac{t}{2}<y<\frac{t}{2}\},\\ \Gamma_{bs} &= \{(0,y)|-\frac{\epsilon}{2}<y<\frac{\epsilon}{2}\},\\ \Gamma_{cl} &= \{(0,y)||y|>\frac{\epsilon}{2}\}.\end{aligned}$$

Let Ω_r , Ω_b and Ω_s denote the domain occupied by the river , the bay and the open sea respectively. Then we have

$$\begin{aligned}\Omega_r &= \{(x,y)|-s-a<x<-a,-\frac{t}{2}<y<\frac{t}{2}\},\\ \Omega_s &= \{(x,y)|x>0\};\end{aligned}$$

* Received January 7, 2002.
1) This work was supported partly by the Special Funds for Major State Basic Research Projects of China and the National Natural Science Foundation of China. Computation was supported by the State Key Lab. of the Scientific and Engineering Computing in China.

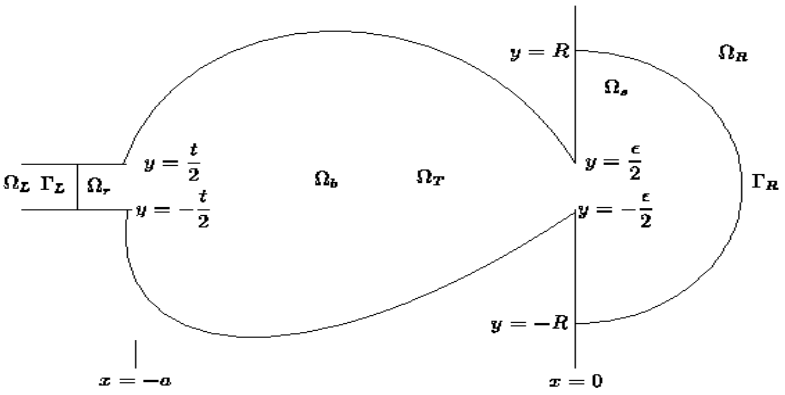

Figure 1: The physical and the computational domain

where s is the length of the river. $s = 0$ represents no river and $s = \infty$ represents a semi-infinite river.

In the following, we only discuss the case $s = \infty$.

The Ω_b can have any shape, Figure 1 shows one applicable choice.

Denote $\Omega_{br} = \Omega_r \cup \Omega_b \cup \Gamma_{rm}$, and $\Gamma_{br} = \partial\Omega_{br} \setminus \Gamma_{bs}$.

We have the following equations and boundary conditions for the complex amplitude of water surface oscillation(cf. [17]):

$$\triangle\eta + (1 + i\xi)^2 k^2 \eta = 0 \qquad \text{in } \Omega_{br}, \tag{1.1}$$

$$\triangle\eta + k^2\eta = 0 \qquad \text{in } \Omega_s, \tag{1.2}$$

$$\frac{\partial\eta}{\partial n} = 0 \qquad \text{on } \Gamma_{br}, \tag{1.3}$$

$$\frac{\partial\eta}{\partial n} = 0 \qquad \text{on } \Gamma_{cl}, \tag{1.4}$$

$$\eta, \frac{\partial\eta}{\partial x} \text{ is continuous} \qquad \text{on } \Gamma_{\text{bs}}, \tag{1.5}$$

$$\lim_{r\to\infty} \sqrt{r}[\frac{\partial(\eta - \eta_0)}{\partial r} - ik(\eta - \eta_0)] = 0, \tag{1.6}$$

$$\begin{aligned}&\text{In the river } \eta \text{ is bounded and}\\ &\text{represents waves that}\\ &\text{propagate in the negative x} - \text{direction;}\end{aligned} \tag{1.7}$$

where η is the complex amplitude of water surface oscillation, of which the modulus and the argument represent the conventional amplitude and the relative phase of the local water surface oscillations, respectively; k denotes wave number; ξ is the resistance coefficient to model the effects of dissipation, in the open sea, dissipativity is generally insignificant, so (1.2) takes (1.1) when $\xi = 0$; $\dfrac{\partial}{\partial n}$ represents outward normal derivative of $\partial\Omega_{br}$ or $\partial\Omega_s$; $r = \sqrt{x^2 + y^2}$ when $x > 0$, condition (1.6) is known as the Sommerfeld radiation condition; η_0 represents the water surface oscillation induced by the incident wave along with the coastline reflection in case of a vanishing bay entrance and, consequently, a continuous coastline. If the incident wave is of a wave height H_0 and is in the direction forming an angle α with the x-axis, then η_0 can be

expressed by (cf. [15])

$$\eta_0 = \frac{H_0}{2} e^{ik(y\sin\alpha - x\cos\alpha)} + \frac{H_0}{2} e^{ik(y\sin\alpha + x\cos\alpha)} = H_0 e^{iky\sin\alpha}\cos(kx\cos\alpha). \tag{1.8}$$

For a special case, the shape of both the bay and river has been extremely simplified, X. Yu [15] employed a method of patching formal expression to obtain the analytic solution of problem (1.1)-(1.7). Furthermore, X. Yu and H. Togashi [16] numerically studed the natural and wave-induced oscillations in Nagasaki Bay, which is a coupled bay-river system. In the paper, a simple no-interference condition is introduced near the mouth of the river to reduce the problem on a bounded computational domain. One difficulty in the numerical simulation of a coupled bay-river system is the unboundedness of the physical domain.

In the past two decades, there have been many important progress in solving partial differential equations in unbounded domains, see, e.g. [2]-[13]. One of the most popular approach is the artificial boundary condition method, which is used to handle the unboundedness of the physical domain of the given problem (1.1)-(1.7) in this paper.

The main purpose of this work is to design a class of high-order artificial boundary conditions for the problem (1.1)-(1.7). We introduce a artificial boundary Γ_R in the open sea and a artificial boundary Γ_L in the river. (see Figure 1). The high-order artificial boundary conditions are then obtained by using the integral of known information on the artificial boundary.

The organization of this paper is as follows. In section 2, we will discuss the artificial boundary conditions on both Γ_R and Γ_L, and reduce the original problem to a problem defined on bounded computational domain. In section 3, we will get the equivalent variational problem for the reduced problem. The efficiency and accuracy of the proposed schemes will be demonstrated by several numerical examples in section 4. Some concluding remarks will be given in the final section.

2. The Artificial Boundary Conditions

To begin with, we first introduce some notations.

We choose $R > \frac{\epsilon}{2}$, introduce an artificial boundary in the open sea as:

$$\Gamma_R = \{(x,y) | x^2 + y^2 = R^2, x > 0\}.$$

Choosing $L < -a$, we define artificial boundary in the river as:

$$\Gamma_L = \{(x,y) | x = L, -\frac{t}{2} < y < \frac{t}{2}\}.$$

Denote $\Omega = \Omega_{br} \cup \Omega_s \cup \Gamma_{bs}$, let

$$\Omega_R = \{(x,y) | x^2 + y^2 > R^2, x > 0\}$$

and

$$\Omega_L = \{(x,y) | x < L, -\frac{t}{2} < y < \frac{t}{2}\}.$$

Then the bounded computational domain Ω_T is:

$$\Omega_T = \Omega \setminus (\overline{\Omega_R} \cup \overline{\Omega_L}).$$

2.1. The Artificial Boundary Conditions on the Artificial Boundary Γ_R in the Open Sea

In this subsection we consider the artificial boundary condition on the artificial boundary Γ_R in the open sea. The restriction of the solution of the problem (1.1)-(1.7) on the domain Ω_R satisfies:

$$\triangle\eta + k^2\eta = 0 \qquad \text{in } \Omega_R, \tag{2.1}$$

$$\frac{\partial\eta}{\partial x} = 0 \qquad \{(0,y)||y| > R\}, \tag{2.2}$$

$$\lim_{r\to\infty}\sqrt{r}[\frac{\partial(\eta-\eta_0)}{\partial r} - ik(\eta-\eta_0)] = 0; \tag{2.3}$$

where η_0 is described in (1.8).

Let

$$\eta' = \eta - \eta_0, \tag{2.4}$$

we can verify that η_0 also satisfies (2.1)-(2.2), so η' satisfies:

$$\triangle\eta' + k^2\eta' = 0 \qquad \text{in } \Omega_R, \tag{2.5}$$

$$\frac{\partial\eta'}{\partial x} = 0 \qquad \{(0,y)||y| > R\}, \tag{2.6}$$

$$\lim_{r\to\infty}\sqrt{r}[\frac{\partial\eta'}{\partial r} - ik\eta'] = 0. \tag{2.7}$$

We can get the general solution of (2.5)-(2.7) by using separation of variables in polar coordinates in the plane:

$$\eta'(r,\theta) = \sum_{m=0}^{\infty} c_m H_m^{(1)}(kr)cos(m(\theta+\frac{\pi}{2})) \qquad r \geq R, -\frac{\pi}{2} \leq \theta \leq \frac{\pi}{2}, \tag{2.8}$$

where $H_m^{(1)}$ is the Hankel function of the first kind and of the m order, $\{c_m\}$ are constants to be determined.

Combining (1.8),(2.8) and (2.4) we have:

$$\begin{aligned}\eta(r,\theta) &= \eta'(r,\theta) + \eta_0(r,\theta)\\ &= \sum_{m=0}^{\infty} c_m H_m^{(1)}(kr)cos(m(\theta+\frac{\pi}{2}))\\ &+ e^{iky\sin\alpha}\cos(kx\cos\alpha)\end{aligned} \tag{2.9}$$

and

$$\begin{aligned}\frac{\partial\eta}{\partial r}\Big|_{\Gamma_R} &= \sum_{m=0}^{\infty} c_m k H_m^{(1)'}(kR)\cos(m(\theta+\frac{\pi}{2}))\\ &+ ik\sin\theta\sin\alpha e^{iky\sin\alpha}\cos(kx\cos\alpha)\\ &- k\cos\theta\cos\alpha e^{iky\sin\alpha}\sin(kx\cos\alpha).\end{aligned} \tag{2.10}$$

We need to find out the expressions for $\{c_m\}$.

The functions $\{\cos(m(\theta+\frac{\pi}{2}))\ \ m = 0,1,\cdots\}$ are orthogonal on $[-\frac{\pi}{2},\frac{\pi}{2}]$:

$$\int_{-\frac{\pi}{2}}^{\frac{\pi}{2}}\cos(k(\theta+\frac{\pi}{2}))\cos(j(\theta+\frac{\pi}{2}))d\theta = 0, \qquad k \neq j.$$

We have:

$$\begin{aligned}\int_{-\frac{\pi}{2}}^{\frac{\pi}{2}} (\eta-\eta_0)|_{\Gamma_R}\cos(m(\theta+\frac{\pi}{2}))d\theta &= c_m H_m^{(1)}(kR)\int_{-\frac{\pi}{2}}^{\frac{\pi}{2}}\cos^2(m(\theta+\frac{\pi}{2}))d\theta \\ &= \begin{cases} \pi c_m H_m^{(1)}(kR) & m=0 \\ \frac{\pi}{2}c_m H_m^{(1)}(kR) & m>0 \end{cases}.\end{aligned}$$

Therefore we have:

$$c_m = \frac{t_m\int_{-\frac{\pi}{2}}^{\frac{\pi}{2}}(\eta-\eta_0)|_{\Gamma_R}\cos(m(\theta+\frac{\pi}{2}))d\theta}{H_m^{(1)}(kR)}, \qquad m\geq 0 \tag{2.11}$$

with

$$t_m = \begin{cases} \frac{1}{\pi} & m=0 \\ \frac{2}{\pi} & m>0 \end{cases}. \tag{2.12}$$

Substitute (2.11) into (2.10), we get:

$$\begin{aligned}\frac{\partial\eta}{\partial r}\Big|_{\Gamma_R} &= \sum_{m=0}^{\infty}\frac{t_m k H_m^{(1)'}(kR)\cos(m(\theta+\frac{\pi}{2}))\int_{-\frac{\pi}{2}}^{\frac{\pi}{2}}(\eta-\eta_0)|_{\Gamma_R}\cos(m(\theta+\frac{\pi}{2}))d\theta}{H_m^{(1)}(kR)} \\ &+ ik\sin\theta\sin\alpha e^{iky\sin\alpha}\cos(kx\cos\alpha) \\ &- k\cos\theta\cos\alpha e^{iky\sin\alpha}\sin(kx\cos\alpha).\end{aligned} \tag{2.13}$$

The condition (2.13) is the exact boundary condition satisfied by the solution η of problem (1.1)-(1.7). Let

$$\begin{aligned}D_R^M(\eta) &= \sum_{m=0}^{M}\frac{t_m k H_m^{(1)'}(kR)\cos(m(\theta+\frac{\pi}{2}))\int_{-\frac{\pi}{2}}^{\frac{\pi}{2}}(\eta-\eta_0)|_{\Gamma_R}\cos(m(\theta+\frac{\pi}{2}))d\theta}{H_m^{(1)}(kR)} \\ &+ ik\sin\theta\sin\alpha e^{iky\sin\alpha}\cos(kx\cos\alpha) \\ &- k\cos\theta\cos\alpha e^{iky\sin\alpha}\sin(kx\cos\alpha)\end{aligned} \tag{2.14}$$

for $M=0,1,2,\cdots$, then we obtain a sequence of approximate artificial boundary conditions on the artificial boundary Γ_R:

$$\frac{\partial\eta}{\partial r}\Big|_{\Gamma_R} = D_R^M(\eta). \tag{2.15}$$

2.2. The Artificial Boundary Conditions on the Artificial Boundary Γ_L in the River

We need to set up proper artificial boundary conditions on the artificial boundary Γ_L in the river.

We consider the restriction of the solution of the problem (1.1)-(1.7) on the domain Ω_L , which satisfies:

$$\triangle\eta + (1+i\xi)^2k^2\eta = 0 \qquad \text{in } \Omega_L, \tag{2.16}$$

$$\frac{\partial\eta}{\partial y} = 0 \qquad \{(x, \pm\frac{t}{2})|x < L\}, \tag{2.17}$$

$$\eta \text{ is bounded and represents waves that propagate in the negative } x-\text{direction;} \tag{2.18}$$

the general solution of (2.16)-(2.18) can be obtained by separation of variables:

$$\eta = \sum_{m=0}^{\infty} a_m e^{\mu_m(x-L)} \cos(\frac{1}{2}+\frac{y}{t})m\pi, \qquad (x,y) \in \overline{\Omega}_L, \tag{2.19}$$

where $\{a_m\}$ are constants to be determined, $\{\mu_m\}$ have the following expression:

$$\mu_m = k[(\frac{m\pi}{kt})^2 - (1+i\xi)^2]^{1/2}, \quad m \geq 0. \tag{2.20}$$

According to condition (2.18), the waves represented by η should propagate in the negative x-direction, so the imaginary part of $\{\mu_m\}$ should be non-positive, since $\xi \geq 0$, we can verify that the real part of $\{\mu_m\}$ is non-negative when the imaginary part of $\{\mu_m\}$ is negative, and we can choose the definition of square root in (2.20) so that the real part of $\{\mu_m\}$ is non-negative when the imaginary part of $\{\mu_m\}$ equals zero. In any situation, we can always choose the definition of square root in (2.20) so that $\{\mu_m\}$ has a non-negative real part and non-positive imaginary part for $m \geq 0$, thus $\{a_m e^{\mu_m(x-L)}\}$ represent non-growing waves propagating in the negative x-direction. By taking this choice, η expressed by (2.19) would then satisfies condition (2.18).

The functions $\{\cos(\frac{1}{2}+\frac{y}{t})m\pi \;\; m = 0, 1, \cdots\}$ are orthogonal on $[-\frac{t}{2}, \frac{t}{2}]$:

$$\int_{-\frac{t}{2}}^{\frac{t}{2}} \cos(\frac{1}{2}+\frac{y}{t})k\pi \cos(\frac{1}{2}+\frac{y}{t})j\pi dy = 0, \qquad k \neq j,$$

then

$$\begin{aligned}\int_{-\frac{t}{2}}^{\frac{t}{2}} \eta|_{\Gamma_L} \cos(\frac{1}{2}+\frac{y}{t})m\pi dy &= a_m \int_{-\frac{t}{2}}^{\frac{t}{2}} \cos^2(\frac{1}{2}+\frac{y}{t})m\pi dy \\ &= \begin{cases} ta_m & m = 0 \\ \frac{t}{2}a_m & m > 0 \end{cases},\end{aligned}$$

so we have:

$$a_m = p_m \int_{-\frac{t}{2}}^{\frac{t}{2}} \eta|_{\Gamma_L} \cos(\frac{1}{2}+\frac{y}{t})m\pi dy, \qquad m \geq 0, \tag{2.21}$$

where

$$p_m = \begin{cases} \frac{1}{t} & m = 0 \\ \frac{2}{t} & m > 0 \end{cases}. \tag{2.22}$$

From (2.19) we have:

$$\frac{\partial \eta}{\partial x}\Big|_{\Gamma_L} = \sum_{m=0}^{\infty} a_m \mu_m \cos(\frac{1}{2} + \frac{y}{t})m\pi, \tag{2.23}$$

substitute (2.21) into (2.23), we have:

$$\frac{\partial \eta}{\partial n}\Big|_{\Gamma_L} = -\frac{\partial \eta}{\partial x}\Big|_{\Gamma_L} = -\sum_{m=0}^{\infty} p_m \mu_m \cos(\frac{1}{2} + \frac{y}{t})m\pi \int_{-\frac{t}{2}}^{\frac{t}{2}} \eta|_{\Gamma_L} \cos(\frac{1}{2} + \frac{y}{t})m\pi dy, \tag{2.24}$$

where $\frac{\partial}{\partial n}$ represents outward normal derivative of $\partial\Omega_T$.

The condition (2.24) is the exact boundary condition satisfied by the solution η of (2.16)-(2.18). Let

$$U_L^N(\eta) = -\sum_{m=0}^{N} p_m \mu_m \cos(\frac{1}{2} + \frac{y}{t})m\pi \int_{-\frac{t}{2}}^{\frac{t}{2}} \eta|_{\Gamma_L} \cos(\frac{1}{2} + \frac{y}{t})m\pi dy \tag{2.25}$$

for $N = 0, 1, \cdots$.

On the artificial boundary Γ_L we obtain a sequence of approximate artificial boundary conditions:

$$\frac{\partial \eta}{\partial n}\Big|_{\Gamma_L} = U_L^N(\eta). \tag{2.26}$$

2.3. The Reduced Boundary Value Problem of Problem (1.1)-(1.7)

Using the artificial boundary conditions given in this section, the problem (1.1)-(1.7) can be reduced to a boundary value problem on the computational domain Ω_T.

We denote

$$\begin{aligned} \Omega_T^{br} &= \Omega_T \cap \Omega_{br}, \\ \Omega_T^{s} &= \Omega_T \cap \Omega_{s}, \\ \Gamma_T^{br} &= \partial\Omega_T^{br} \setminus \Gamma_{bs}, \\ \Gamma_T^{cl} &= \Gamma_{cl} \cap \{(0, y) | |y| \le R\}. \end{aligned}$$

The reduced boundary value problem is:

$$\triangle\eta + (1 + i\xi)^2 k^2 \eta = 0 \qquad \text{in } \Omega_T^{br}, \tag{2.27}$$

$$\triangle\eta + k^2\eta = 0 \qquad \text{in } \Omega_T^{s}, \tag{2.28}$$

$$\frac{\partial \eta}{\partial n} = 0 \qquad \Gamma_T^{br} \setminus \Gamma_L, \tag{2.29}$$

$$\frac{\partial \eta}{\partial n} = U_L^N(\eta) \qquad \Gamma_L, \tag{2.30}$$

$$\frac{\partial \eta}{\partial n} = 0 \qquad \Gamma_T^{cl}, \tag{2.31}$$

$$\eta, \frac{\partial \eta}{\partial x} \text{ is continuous} \qquad \text{on } \Gamma_{\rm bs}, \tag{2.32}$$

$$\frac{\partial \eta}{\partial r} = D_R^M(\eta) \qquad \Gamma_R. \tag{2.33}$$

In the following section the equivalent variational problem of the reduced problem (2.27)-(2.33) will be given.

3. The Equivalent Variational Problem of Problem (2.27)-(2.33)

In this section the equivalent variational problem for the problem (2.27)-(2.33) will be proposed. Let $H^m(\Omega_T)$ denote the usual Sobolev spaces on the domain Ω_T with integer m , cf. [1].

From (2.27) we have:

$$\int_{\Omega_T^{br}} \nabla\eta\nabla\zeta dxdy - \int_{\Omega_T^{br}} k^2(1+i\xi)^2\eta\zeta dxdy = \int_{\Gamma_{bs}} \frac{\partial\eta}{\partial n}\zeta dy + \int_{\Gamma_L} \frac{\partial\eta}{\partial n}\zeta dy \quad \forall\zeta \in H^1(\Omega_T), \quad (3.1)$$

where η is the solution of problem (2.27)-(2.33); $\dfrac{\partial}{\partial n}$ represents outward normal derivative of $\partial\Omega_T^{br}$.

From (2.28) we have:

$$\int_{\Omega_T^{s}} \nabla\eta\nabla\zeta dxdy - \int_{\Omega_T^{s}} k^2\eta\zeta dxdy = \int_{\Gamma_{bs}} \frac{\partial\eta}{\partial n}\zeta dy + \int_{\Gamma_R} \frac{\partial\eta}{\partial n}\zeta d\theta \quad \forall\zeta \in H^1(\Omega_T), \quad (3.2)$$

where $\dfrac{\partial}{\partial n}$ represents outward normal derivative of $\partial\Omega_T^{s}$.

Adding (3.1) and (3.2), and noting $\dfrac{\partial\eta}{\partial x}$ is continuous on Γ_{bs}, we get:

$$\begin{aligned} &\int_{\Omega_T} \nabla\eta\nabla\zeta dxdy - \int_{\Omega_T^{br}} k^2(1+i\xi)^2\eta\zeta dxdy - \int_{\Omega_T^{s}} k^2\eta\zeta dxdy \\ = &\int_{\Gamma_L} \frac{\partial\eta}{\partial n}\zeta dy + \int_{\Gamma_R} \frac{\partial\eta}{\partial n}\zeta d\theta \qquad \forall\zeta \in H^1(\Omega_T), \end{aligned} \quad (3.3)$$

where $\dfrac{\partial}{\partial n}$ represents outward normal derivative of $\partial\Omega_T$.

Substituting (2.26) and (2.15) into (3.3), we can get the equivalent variational problem of problem (2.27)-(2.33):

$$\text{Find } \eta \in H^1(\Omega_T), \text{ such that}$$

$$A_{MN}^1(\eta,\zeta) = F(\zeta), \quad \forall\zeta \in H^1(\Omega_T), \quad (3.4)$$

where

$$\begin{aligned} A_{MN}^1(\eta,\zeta) &= A_T(\eta,\zeta) + A_L(\eta,\zeta) + A_R(\eta,\zeta), \\ A_T(\eta,\zeta) &= \int_{\Omega_T} \nabla\eta\nabla\zeta dxdy - \int_{\Omega_T^{br}} k^2(1+i\xi)^2\eta\zeta dxdy - \int_{\Omega_T^{s}} k^2\eta\zeta dxdy, \\ A_L(\eta,\zeta) &= \sum_{m=0}^{N} p_m\mu_m \int_{-\frac{t}{2}}^{\frac{t}{2}} \zeta|_{\Gamma_L}\cos(\frac{1}{2}+\frac{y}{t})m\pi dy \int_{-\frac{t}{2}}^{\frac{t}{2}} \eta|_{\Gamma_L}\cos(\frac{1}{2}+\frac{y}{t})m\pi dy, \end{aligned}$$

$$A_R(\eta,\zeta) = -\sum_{m=0}^{M} \frac{t_m kRH_m^{(1)'}(kR)\int_{-\frac{\pi}{2}}^{\frac{\pi}{2}} \eta|_{\Gamma_R}\cos(m(\theta+\frac{\pi}{2}))d\theta \int_{-\frac{\pi}{2}}^{\frac{\pi}{2}} \zeta|_{\Gamma_R}\cos(m(\theta+\frac{\pi}{2}))d\theta}{H_m^{(1)}(kR)},$$

$$F(\zeta) = -\sum_{m=0}^{M} \frac{t_m kRH_m^{(1)'}(kR)\int_{-\frac{\pi}{2}}^{\frac{\pi}{2}} \eta_0|_{\Gamma_R}\cos(m(\theta+\frac{\pi}{2}))d\theta \int_{-\frac{\pi}{2}}^{\frac{\pi}{2}} \zeta|_{\Gamma_R}\cos(m(\theta+\frac{\pi}{2}))d\theta}{H_m^{(1)}(kR)}$$

$$+R\int_{-\frac{\pi}{2}}^{\frac{\pi}{2}} ik\sin\theta\sin\alpha e^{ikR\sin\theta\sin\alpha}\cos(kR\cos\theta\cos\alpha)\zeta d\theta$$

$$-R\int_{-\frac{\pi}{2}}^{\frac{\pi}{2}} k\cos\theta\cos\alpha e^{ikR\sin\theta\sin\alpha}\sin(kR\cos\theta\cos\alpha)\zeta d\theta.$$

Remark. When there is no river or the river has finite length, we would perform the perfect reflective condition in the end of river, thus we only need to use the artificial boundary conditions (2.15) to reduce the original problem to a problem on a finite computational domain. The deductive method is similar, so we only list the equivalent variational problem for this case in the following:

$$\text{Find } \eta \in H^1(\Omega_T), \text{ such that}$$

$$A_M^2(\eta,\zeta) = F(\zeta), \qquad \forall\zeta \in H^1(\Omega_T), \tag{3.5}$$

where

$$A_M^2(\eta,\zeta) = A_T(\eta,\zeta) + A_R(\eta,\zeta).$$

4. Numerical Results

In the following numerical examples, the domain Ω_T is divided into small triangles. Let V_h denote the standard finite element subspace of $H^1(\Omega_T)$ by the linear elements. Namely

$$V_h = \{v_h | v_h \in C^0(\overline{\Omega_T}) \text{ and on each triangle } v_h \text{ is a linear function}\}.$$

Then we obtain the finite element approximation of the problem (3.4) :

$$\text{Find } \eta_h \in V_h, \text{ such that}$$

$$A_{MN}^1(\eta_h,\zeta_h) = F(\zeta_h), \qquad \forall\zeta_h \in V_h, \tag{4.1}$$

and the finite element approximation of the problem (3.5):

$$\text{Find } \eta_h \in V_h, \text{ such that}$$

$$A_M^2(\eta_h,\zeta_h) = F(\zeta_h), \qquad \forall\zeta_h \in V_h. \tag{4.2}$$

After solving the problem (4.1) or (4.2) we obtain the approximate solution η_h of the original problem (1.1)-(1.7) on the computational domain Ω_T.

In this section, we first present a numerical experiment which demonstrate the effectiveness of the artificial boundary condition, then we will calculate numerical solution of the problem (1.1)-(1.7) and the relations between amplification factor and wave number, finally, we will test the effect of choosing different terms in the artificial boundary condition and choosing different location of the artificial boundary.

We will calculate problem (4.1) or (4.2) for two different shapes of the bay.

Let

$$\begin{aligned}
\Omega_b^1 &= \{(x,y)| -a < x < 0, -\frac{b}{2} < y < \frac{b}{2}\},\\
\Omega_b^2 &= \{(x,y)| -a < x < 0, -\frac{b}{2} < y < \frac{b}{2}\}\\
&\cup \{(x,y)| y \geq \frac{b}{2}, (x+\frac{a}{2})^2 + (y-\frac{b}{2})^2 < \frac{a^2}{4}\}\\
&\cup \{(x,y)| y \leq -\frac{b}{2}, (x+\frac{a}{2})^2 + (y+\frac{b}{2})^2 < \frac{a^2}{4}\}.
\end{aligned}$$

When calculate with Ω_b^1, we choose $a = 12, b = 5, \epsilon = 1, t = 1, R = 2.5$, three meshes are employed in our computations in this case. For a given mesh, the mesh size h is defined as the maximum of the border-lengths of all triangles in the mesh. Figure 2 shows the partition for mesh A(h=0.25) of Ω_T. We can see in this case, some nodes in Ω_T^{br} have the same position with the other nodes in Ω_T^s. Mesh B(h=0.125) is generated by dividing each triangle in mesh A into four equal smaller triangles. Mesh C (h=0.0625) is obtained from mesh B in a similar way.

When calculate with Ω_b^2, we choose $a = 4, b = 1, \epsilon = 1, t = 1, R = 2.5$, two meshes are employed in our computations in this case. Figure 3 shows the partition for mesh A′(h=0.25) of Ω_T. Mesh B′(h=0.125) is generated by dividing each triangle in mesh A′ into four equal smaller triangles.

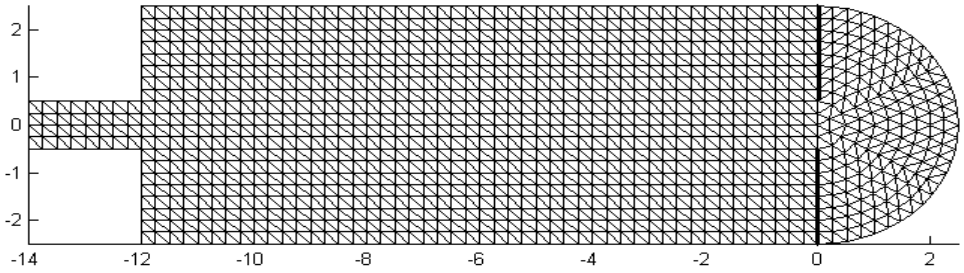

Figure 2: Mesh A

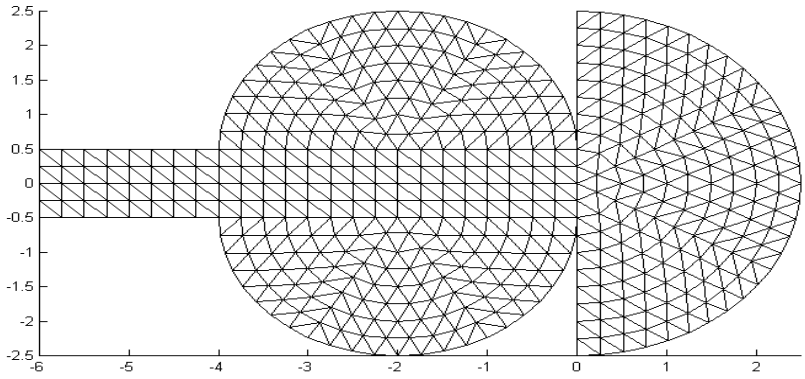

Figure 3: Mesh A′

4.1. Numerical Results of a Test Problem

We consider the case no river is present.

Let

$$\eta_1 = e^{iky\sin\alpha}\cos(kx\cos\alpha),$$

consider following boundary value problem which is similar to problem (2.27)-(2.33):

$$\triangle\eta + k^2\eta = 0 \qquad \text{in } \Omega_T, \tag{4.3}$$

$$\frac{\partial \eta}{\partial n} = \frac{\partial \eta_1}{\partial n} \qquad \Gamma_T^{br}, \tag{4.4}$$

$$\frac{\partial \eta}{\partial n} = 0 \qquad \Gamma_T^{cl}, \tag{4.5}$$

$$\frac{\partial \eta}{\partial r} = D_R^M(\eta) \qquad \Gamma_R; \tag{4.6}$$

where $\dfrac{\partial}{\partial n}$ is the outward normal derivative of $\partial\Omega_T$.

It can be verified that η_1 is the exact solution of the problem (4.3)-(4.6). It can also be verified that the Problem (4.3)-(4.6) is equivalent to the following variational problem:

$$\text{Find } \eta \in H^1(\Omega_T), \text{ such that}$$

$$\widetilde{A}_T(\eta,\zeta) + A_R(\eta,\zeta) = F(\zeta) + \widetilde{F}(\zeta), \qquad \forall\, \zeta \in H^1(\Omega_T), \tag{4.7}$$

where $A_R(\eta,\zeta), F(\zeta)$ is described in section 3 and

$$\begin{aligned} \widetilde{A}_T(\eta,\zeta) &= \int_{\Omega_T} \nabla\eta\nabla\zeta dxdy - \int_{\Omega_T} k^2\eta\zeta dxdy, \\ \widetilde{F}(\zeta) &= \int_{\Gamma_R} \frac{\partial \eta_1}{\partial n}\zeta ds. \end{aligned}$$

It can be verified that $\widetilde{A}_T(\eta,\zeta)$ is the same as $A_T(\eta,\zeta)$ when $\xi = 0$. In this case, (4.7) and (3.5) have the same bilinear form.

We choose Ω_b^1 as the shape of the bay. By using our finite element method, a numerical solution η_h of variational problem (4.7) is obtained. The relative errors of $\eta_h - \eta_1$ in L_∞-, L_2- and H^1-norm are given in the Table 1 for mesh A, B, C, respectively.

Table 1: comparison of η_h with η_1

Errors	$h = 0.25$	$h = 0.125$	$h = 0.0625$
$\max\lvert\eta_h - \eta_1\rvert / \max\lvert\eta_1\rvert$	11.61%	4.71%	0.57%
$\lVert\eta_h - \eta_1\rVert_{0,\Omega_T} / \lVert\eta_1\rVert_{0,\Omega_T}$	5.72%	2.37%	0.29%
$\lVert\eta_h - \eta_1\rVert_{1,\Omega_T} / \lVert\eta_1\rVert_{1,\Omega_T}$	6.57%	3.51%	1.83%

As shown in Table 1, η_h tends to η_1 when the mesh size h decreases. The results demonstrate our artificial boundary conditions are very effective. When use our artificial boundary condition to solve problem in a unbounded domain, the convergence rate of the mesh size is consistent with the usual finite element error estimation for the problems in a bounded domain.

4.2. Numerical Results of Problem (1.1)-(1.7)

We can obtain approximate solution η_h of problem (1.1)-(1.7) by computing problem (4.1) or (4.2).

We have mentioned before the wave amplitude H is the modulus of complex amplitude η, the amplitude factor is then H/H_0. Figures 4-6 show some results of the amplitude factor on mesh B when $k = 0.8333$, for different case of river or ξ .

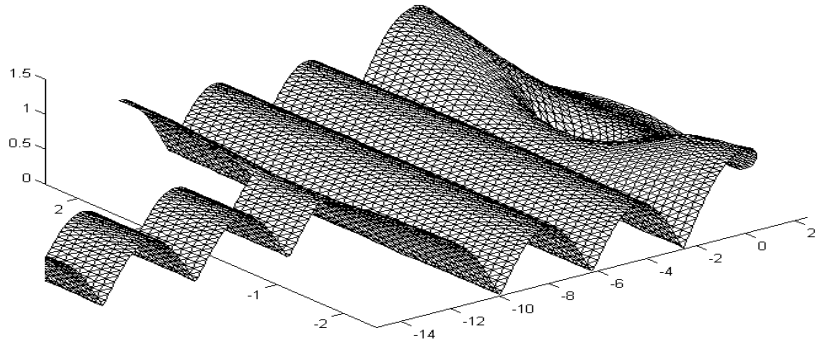

Figure 4: Wave amplification factor with $\xi = 0$ on mesh B. An enclosed river with $s/a = 10$ is present

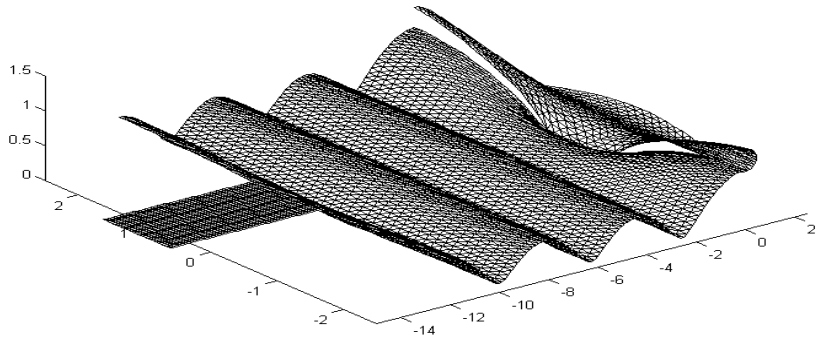

Figure 5: Wave amplification factor with $\xi = 0$ on mesh B. A semi-infinite river is present

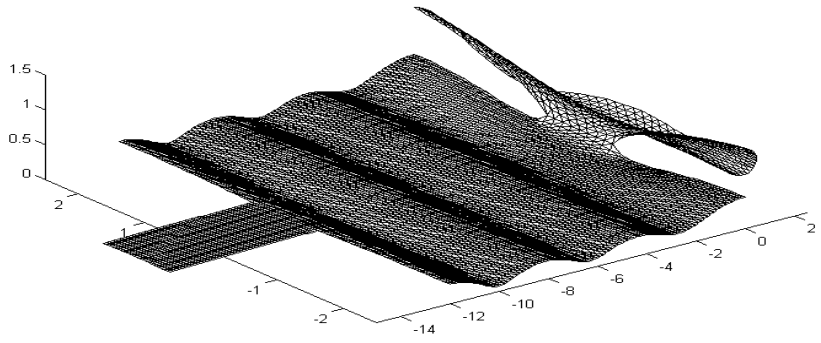

Figure 6: Wave amplification factor with $\xi = 0.05$ on mesh B. A semi-infinite river is present

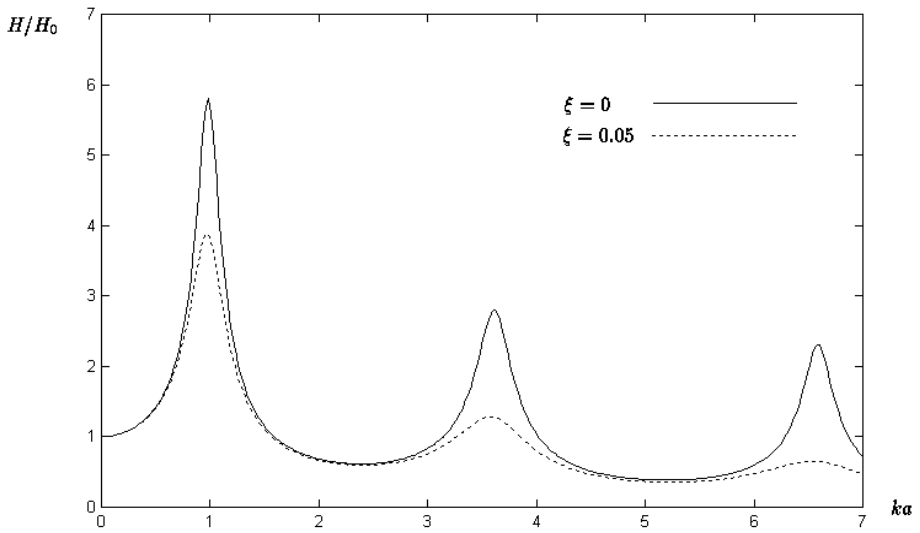

Figure 7: Wave-number response of amplification factor in the bay at $x = -a$ and $y = b/2$ on mesh A for $\xi = 0,\ 0.05$ respectively. No river is present

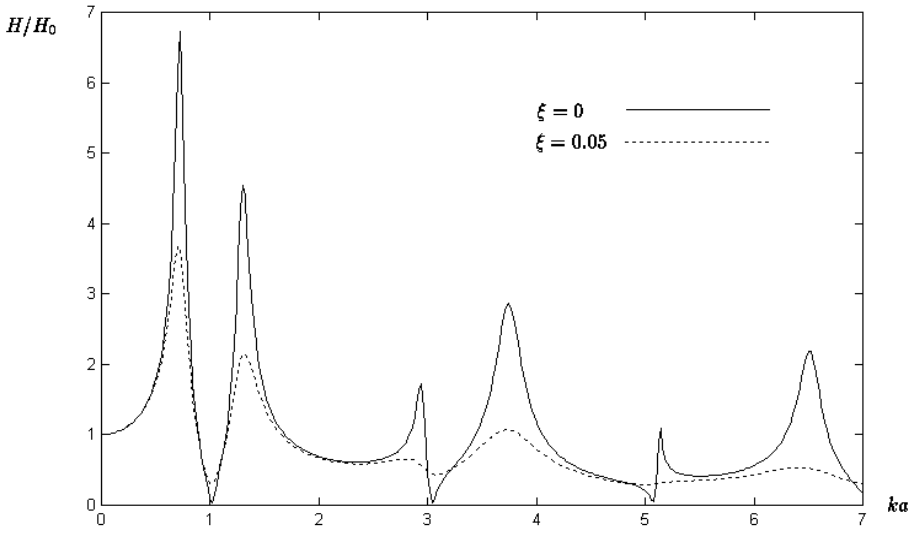

Figure 8: Wave-number response of amplification factor in the bay at $x = -a$ and $y = b/2$ on mesh A for $\xi = 0,\ 0.05$ respectively. An enclosed river with $s/a = 1.5$ is present

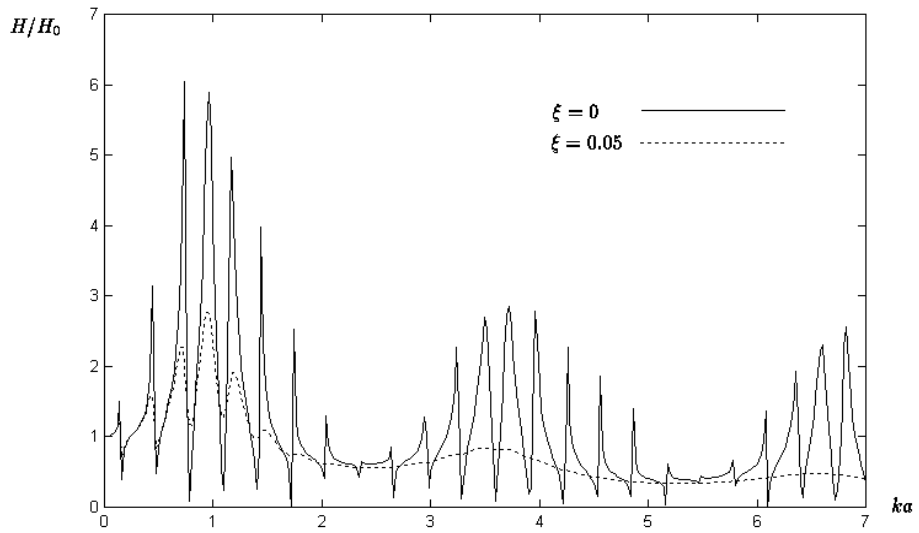

Figure 9: Wave-number response of amplification factor in the bay at $x = -a$ and $y = b/2$ on mesh A for $\xi = 0,\ 0.05$ respectively. An enclosed river with $s/a = 10$ is present

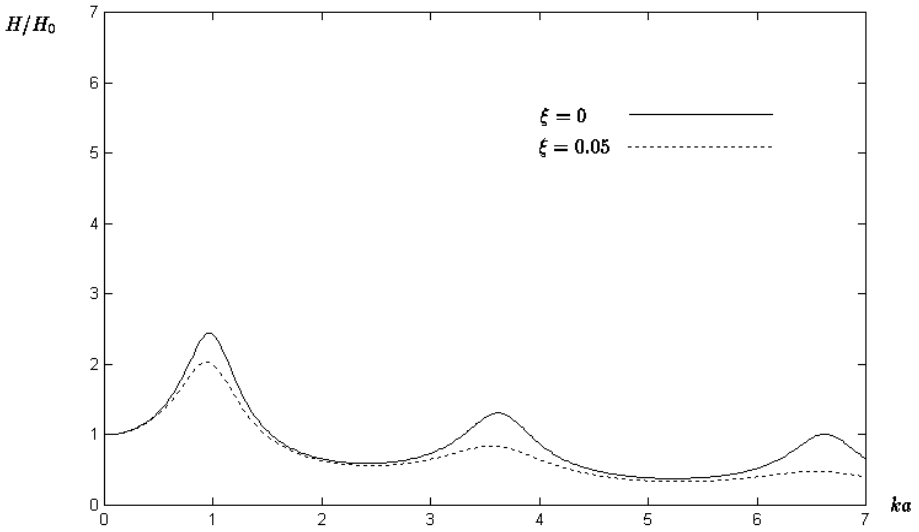

Figure 10: Wave-number response of amplification factor in the bay at $x = -a$ and $y = b/2$ on mesh A for $\xi = 0,\ 0.05$ respectively. A semi-infinite river is present

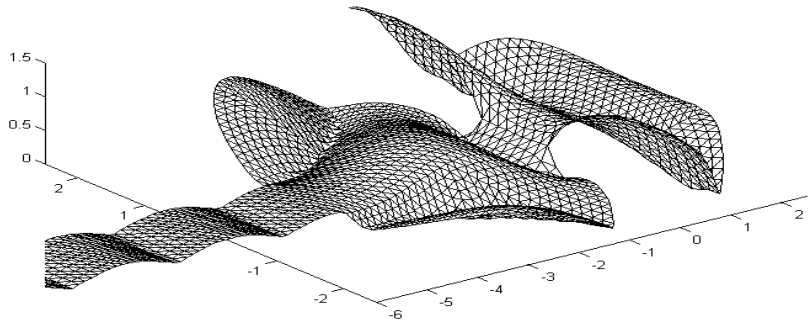

Figure 11: Wave amplification factor with $\xi = 0$ on mesh B$'$. An enclosed river with $s/a = 10$ is present

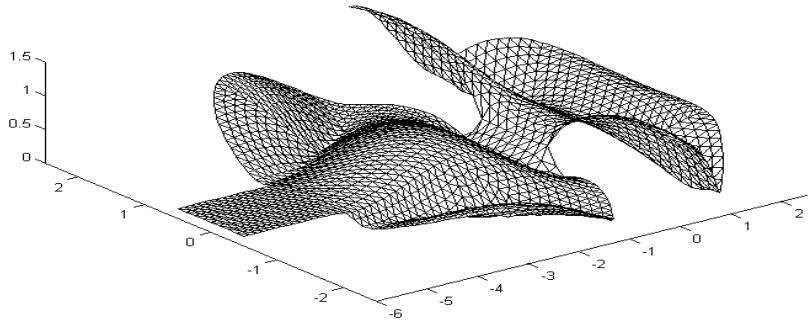

Figure 12: Wave amplification factor with $\xi = 0$ on mesh B$'$. A semi-infinite river is present

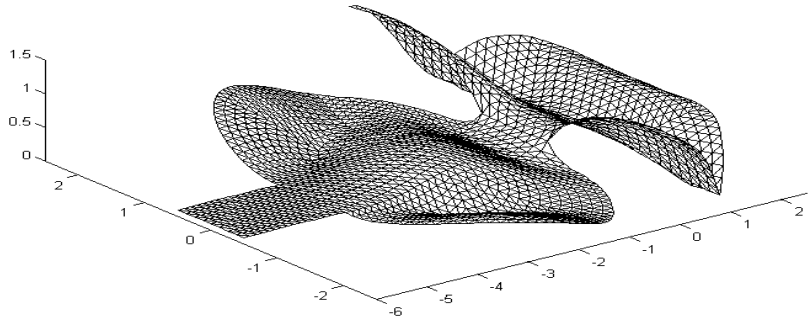

Figure 13: Wave amplification factor with $\xi = 0.05$ on mesh B$'$. A semi-infinite river is present

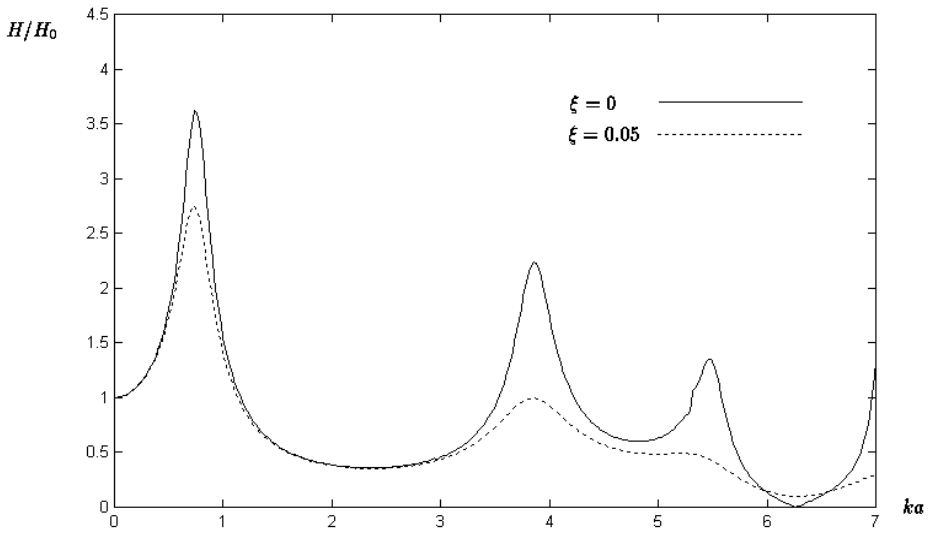

Figure 14: Wave-number response of amplification factor in the bay at $x = -a$ and $y = -b/2$ on mesh A$'$ for $\xi = 0,\ 0.05$ respectively. No river is present

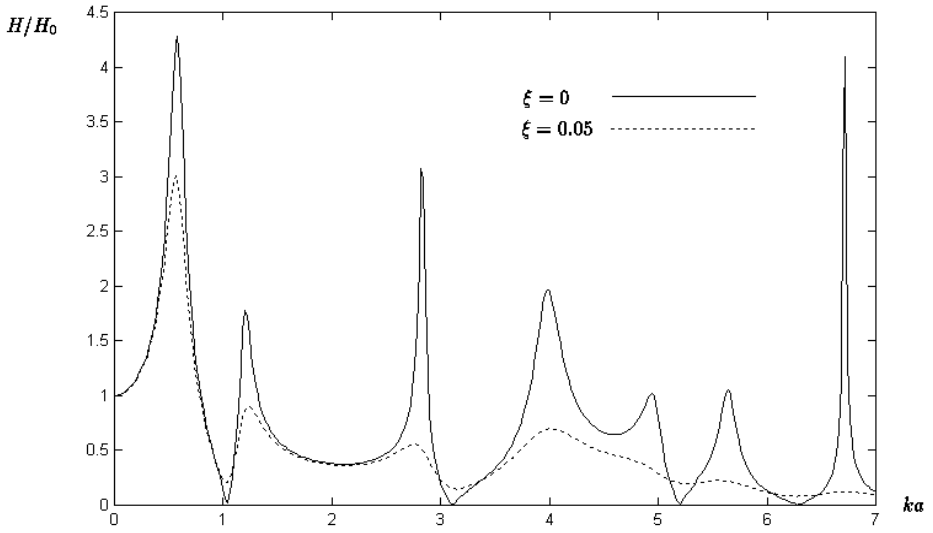

Figure 15: Wave-number response of amplification factor in the bay at $x = -a$ and $y = -b/2$ on mesh A$'$ for $\xi = 0,\ 0.05$ respectively. An enclosed river with $s/a = 1.5$ is present

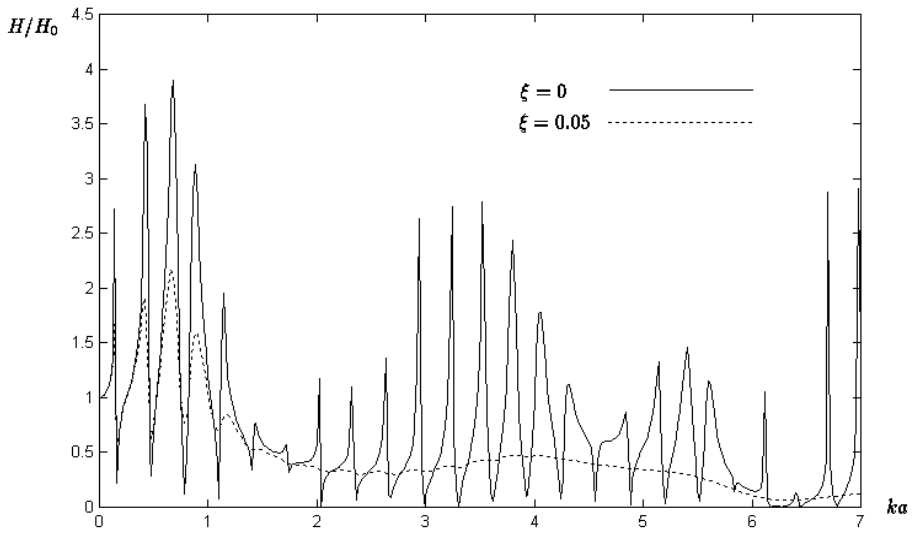

Figure 16: Wave-number response of amplification factor in the bay at $x = -a$ and $y = -b/2$ on mesh A$'$ for $\xi = 0,\ 0.05$ respectively. An enclosed river with $s/a = 10$ is present

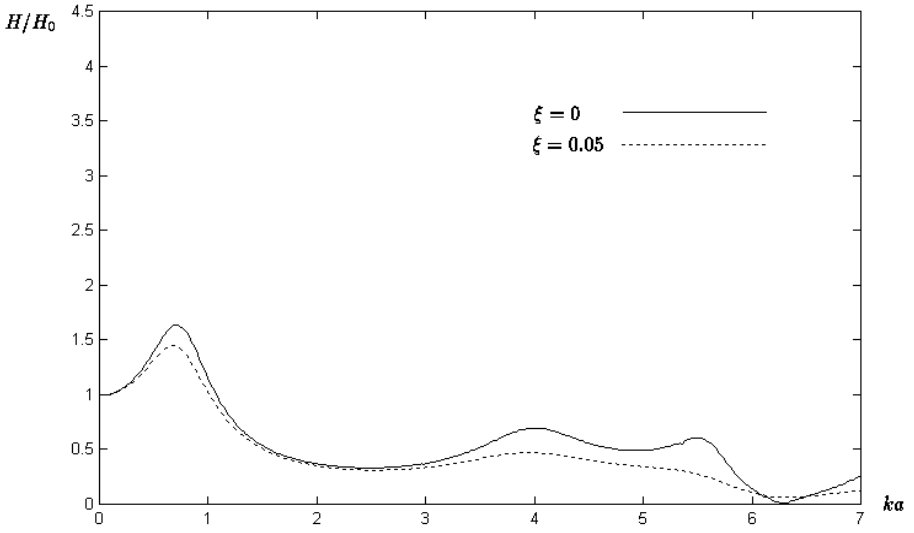

Figure 17: Wave-number response of amplification factor in the bay at $x = -a$ and $y = -b/2$ on mesh A$'$ for $\xi = 0,\ 0.05$ respectively. A semi-infinite river is present

Table 2: The effect for M in the artificial boundary conditions $k = 0.8333$ $\xi = 0$

Errors	$M=0$	$M=2$	$M=4$	$M=6$	$M=10$	$M=20$
$\max\|\eta_h^{100} - \eta_h^M\|$	2.3912E-2	3.3004E-3	2.2238E-3	1.5179E-3	9.9754E-4	3.3969E-4
$\|\eta_h^{100} - \eta_h^M\|_{0,\Omega_T}$	2.8435E-2	1.212E-3	6.1579E-4	3.2517E-4	2.1312E-4	8.4854E-5
$\|\eta_h^{100} - \eta_h^M\|_{1,\Omega_T}$	2.2032E-1	2.4534E-2	1.7445E-2	1.3732E-2	1.1141E-2	5.8338E-3

Table 3: The effect for M in the artificial boundary conditions $k = 0.8333$ $\xi = 0.05$

Errors	$M=0$	$M=2$	$M=4$	$M=6$	$M=10$	$M=20$
$\max\|\eta_h^{100} - \eta_h^M\|$	1.4432E-2	3.1427E-3	2.0188E-3	1.4237E-3	9.0045E-4	3.2239E-4
$\|\eta_h^{100} - \eta_h^M\|_{0,\Omega_T}$	1.6245E-2	1.1096E-3	5.0729E-4	3.1452E-4	1.8375E-4	8.1391E-5
$\|\eta_h^{100} - \eta_h^M\|_{1,\Omega_T}$	1.4315E-1	2.2541E-2	1.5321E-2	1.2621E-2	9.7451E-3	5.2347E-3

Table 4: The effect for M in the artificial boundary conditions $k = 0.4167$ $\xi = 0$

Errors	$M=0$	$M=2$	$M=4$	$M=6$	$M=10$	$M=20$
$\max\|\eta_h^{100} - \eta_h^M\|$	4.7352E-3	5.9373E-4	5.1315E-4	2.9728E-4	2.2965E-4	6.8783E-5
$\|\eta_h^{100} - \eta_h^M\|_{0,\Omega_T}$	5.4331E-3	2.0967E-4	1.9474E-4	7.8812E-5	6.4291E-5	2.1572E-5
$\|\eta_h^{100} - \eta_h^M\|_{1,\Omega_T}$	4.1236E-2	5.1109E-3	5.3374E-3	3.4231E-3	3.2236E-3	1.5297E-3

Table 5: The effect for M in the artificial boundary conditions $k = 0.4167$ $\xi = 0.05$

Errors	$M=0$	$M=2$	$M=4$	$M=6$	$M=10$	$M=20$
$\max\|\eta_h^{100} - \eta_h^M\|$	4.5124E-3	5.7518E-4	4.9804E-4	2.9035E-4	2.2296E-4	6.7325E-5
$\|\eta_h^{100} - \eta_h^M\|_{0,\Omega_T}$	5.2256E-3	2.0219E-4	1.8817E-4	7.7117E-5	6.2243E-5	2.1182E-5
$\|\eta_h^{100} - \eta_h^M\|_{1,\Omega_T}$	3.9321E-2	5.3345E-3	4.9256E-3	3.3475E-3	3.1200E-3	1.4234E-3

Table 6: The effect for M in the artificial boundary conditions $k = 0.2778$ $\xi = 0$

Errors	$M=0$	$M=2$	$M=4$	$M=6$	$M=10$	$M=20$
$\max\|\eta_h^{100} - \eta_h^M\|$	1.4247E-3	1.8916E-4	1.9448E-4	1.2495E-4	1.0963E-4	3.2266E-5
$\|\eta_h^{100} - \eta_h^M\|_{0,\Omega_T}$	1.9345E-3	8.5595E-5	6.6155E-5	3.5769E-5	3.2821E-5	1.1184E-5
$\|\eta_h^{100} - \eta_h^M\|_{1,\Omega_T}$	1.4262E-2	2.2326E-3	2.1007E-3	1.7353E-3	1.6247E-3	7.8243E-4

Table 7: The effect for M in the artificial boundary conditions $k = 0.2778$ $\xi = 0.05$

Errors	$M=0$	$M=2$	$M=4$	$M=6$	$M=10$	$M=20$
$\max\|\eta_h^{100} - \eta_h^M\|$	4.9233E-4	1.5626E-4	1.7609E-4	1.1003E-4	9.2000E-5	2.777E-5
$\|\eta_h^{100} - \eta_h^M\|_{0,\Omega_T}$	7.0730E-4	7.1564E-5	6.1769E-5	3.1954E-5	2.7514E-5	9.7988E-6
$\|\eta_h^{100} - \eta_h^M\|_{1,\Omega_T}$	5.3999E-3	1.8852E-3	1.8175E-3	1.4292E-3	1.3612E-3	6.422E-4

We will calculate the amplification factor for different wave number. Figures 7-10 show the relations between amplification factor H/H_0 at $x = -a$ and $y = b/2$ with the relative wave number ka when $\xi = 0$, 0.05 with no river , enclosed river with different length , and semi-infinite river respectively. Calculations are performed on mesh A. These results are in good

agreement with results found in the literature [15].

Figures 11-13 show some results of the amplitude factor on mesh B′ when $k = 1.5$, for different case of river or ξ.

Figures 14-17 show the relations between amplification factor H/H_0 at $x = -a$ and $y = -b/2$ with the relative wave number ka when $\xi = 0, 0.05$ with no river , enclosed river with different length , and semi-infinite river respectively. Calculations are performed on mesh A′.

4.3. Test of Artificial Boundary Condition on Γ_R

We choose the shape of the bay as Ω_b^1 to perform the numerical test.

We will first test the effect of choosing different terms in the artificial boundary condition. Consider the case no river is present. We will test the effect for different M used in artifical boundary condition on Γ_R. Let η_h^M denote the finite element solution of the problem (4.2), where M is the number used in the bilinear form $A_R(\eta, \zeta)$ and linear form $F(\zeta)$. $M+1$ represents the terms used in artificial boundary condition. Tables 2-7 show the maximum error of $\eta_h^{100} - \eta_h^M$ over mesh points, $\| \eta_h^{100} - \eta_h^M \|_{0,\Omega_T}$ and $\|\eta_h^{100} - \eta_h^M\|_{1,\Omega_T}$ for mesh B with $k = 0.8333, 0.4167$ and $0.2778, \xi = 0, 0.05$, respectively.

As shown in Tables 2-7, the error caused by using different terms in the artificial boundary condition is very small, this means the artificial boundary condition on Γ_R is a good approximation to the exact boundary condition even if M is small. Therefore in the computation very few terms in the bilinear form $A_R(\eta, \zeta)$ and linear form $F(\zeta)$ are only needed in order to get good accuracy.

We will then test the effect of choosing different location of the artificial boundary Γ_R. Still consider the case no river is present. We take $R = 2, 2.5, 3$ and 3.5, respectively. For each R, we use a corresponding mesh with the mesh size h=0.125. Let η denote the finite element solution of (4.2) when $R = 3.5$ and $M = 10$. Table 8 show the maximum error of $\eta - \eta_h^{10}$ over mesh points in Ω_T^{br}, $\|\eta - \eta_h^{10}\|_{0,\Omega_T^{br}}$ and $\|\eta - \eta_h^{10}\|_{1,\Omega_T^{br}}$ for different location of the aitificial boundary Γ_R.

Table 8: The effect of the location of the artificial boundary Γ_R

Errors	$R = 2$	$R = 2.5$	$R = 3$
$\max \lvert\eta - \eta_h^{10}\rvert$	2.0055E-3	9.3841E-4	1.7580E-4
$\|\eta - \eta_h^{10}\|_{0,\Omega_0}$	7.4046E-3	3.5122E-3	6.4931E-4
$\|\eta - \eta_h^{10}\|_{1,\Omega_0}$	3.38E-2	1.5827E-2	3.009E-3

As shown in table 8, the influents caused by choosing different location of artificial boundary Γ_R is very small. This means the artificial boundary condition on Γ_R always has high accuracy wherever the artificial boundary Γ_R is located. Therefore for a given accuracy, it is possible to use a small bounded computational domain to save computational cost.

5. Conclusions

A sequence of high-order artificial boundary conditions at the artificial boundaries in the open sea and the river are designed for the complex amplitude problem in the coupled bay-river system. Then the original problem is reduced to a problem defined on a finite computational

domain, which is equivalent to a variational problem. The variational problem can be solved by finite element method. Then the numerical approximation for the original problem is obtained. Numerical examples show that our artificial boundary conditions are very effective. Summarizing this paper, we can make some conclusions on our method:

- Our artificial boundary conditions are very effective, with this method, the finite element approximate solution have high accuracy and only a few terms in the artificial boundary conditions are needed in computation.
- The convergence rate of the mesh size is consistent with the usual finite element error estimation for the problems in a bounded domain when using our artificial boundary conditions to solve a problem in an unbounded domain.
- The influents caused by different location of artificial boundary Γ_b is very small. Therefore we can choose a small bounded computational domain to get high accuracy.

References

[1] R.A. Adams, Sobolev Spaces, New York: Academic Press., 1975.

[2] B. Engquist and A. Majda, Absorbing boundary conditions for the numerical simulation of waves, *Math. Comp.*, **31** (1977), 629-651.

[3] K. Feng, Asymptotic radiation conditions for reduced wave equations, *J. Comput. Math.*, **2** (1984), 130-138.

[4] D. Givoli, Numerical Methods for Problems in Infinite Domains, Elsevier, Amsterdam, 1992.

[5] C.I. Goldstein, A finite element method for solving Helmholtz type equations in waveguides and other unbounded domains, *Math. Comp.*, **39** (1982), 309-324.

[6] T.M. Hagstrom and H.B. Keller, Exact boundary conditions at artificial boundary for partial differential equations in cylinders, *SIAM J. Math. Anal.*, **17** (1986), 322-341.

[7] T.M. Hagstrom and H.B. Keller, Asymptotic boundary conditions and numerical methods for nonlinear elliptic problems on unbounded domains, *Math. Comp.*, **48** (1987), 449-470.

[8] L. Halpern and M. Schatzman, Artificial boundary conditions for incompressible viscous flows, *SIAM J. Math. Anal.*, **20** (1989), 308-353.

[9] H. Han and W. Bao, An artificial boundary condition for two-dimensional incompressible viscous flows using the method of lines, *Int. J. Numer. Methods Fluids,* **22** (1996), 483-493.

[10] H. Han and W. Bao, An artificial boundary condition for the incompressible viscous flows in a no-slip channel, *J. Comput. Math.,* **13** (1995), 51-63.

[11] H. Han, J. Lu and W. Bao, A discrete artificial boundary condition for steady incompressible viscous flows in a no-slip channel using a fast iterative method, *J. Comput. Phys.*, **114** (1994), 201-208.

[12] H. Han and X. Wu, Approximation of infinite boundary condition and its application to finite element method, *J. Comput. Math.,* **3** (1985), 179-192.

[13] H. Han and X. Wu, The approximation of exact boundary condition at an artificial boundary for linear elastic equation and its application, *Math. Comp.*, **59** (1992), 21-27.

[14] G. B. Whitham, Linear and nonlinear waves, Wiley-Interscience, New York, 1974.

[15] Xiping Yu, Oscillations in a coupled bay-river system. 1. Analytic solution, Coastal Engineering, **28** (1996) 147-164.

[16] Xiping Yu and Hiroyoshi Togashi, Oscillations in a coupled bay-river system, 2, Numerical method, Coastal Engineering, **28** (1996) 165-182.

[17] Xiping Yu and Hiroyoshi Togashi, Irregular waves over and elliptic shoal, Coastal Engineering, **28** (1996) 165-182.